

MESHING ANALYSIS IN CASE OF NONCIRCULAR GEARS DESIGNED FOR THE NAILS FORMING KINEMATICS OPTIMIZATION

Mircea NICULESCU, Laurenția ANDREI

University "Dunărea de Jos" of Galați, Faculty of Engineering, Romania
landrei@ugal.ro

ABSTRACT

Industrial applications often require a variable output motion of mechanisms; noncircular gears are, nowadays, a competitive alternative to electrical devices as providers of variable motion. The authors propose noncircular gear pairs that would modify the kinematics of the crank-slider mechanism of a nail machine, in order to improve the quality of the products. In the attempt of optimizing the nail forming process, two variable slider motions and gear transmission ratios, respectively, are defined. Variation of the gear transmission ratio leads to variation of the noncircular gear geometry, with consequences on gear performances. The paper presents a study of the static tooth contact pattern of the noncircular gears, as a qualitative criterion of the gears meshing, analyzing the influence the modifications in mechanism's kinematics and gears geometry, respectively, have on the gear tooth contact. AutoCAD facilities are used to simulate the gears meshing and to illustrate the tooth contact pattern in static conditions, as a first step in the noncircular gears performances analysis.

Keywords: noncircular gears, nail forming kinematics, gear mesh

1. INTRODUCTION

Noncircular gears keep challenging the specialists due to their design, manufacture and use, approached by different methods as software applications and technology have been improved. As substitute of complex mechanisms and electromotors, the noncircular gears exhibit simplicity, motion accuracy and energetic efficiency. The flexibility of the noncircular gears design, related to a high variety of output functions, assures a continuous source of inspiration for the gears specialists.

The modified crank-slider mechanism, using noncircular gears, has been subject of few applications. Doedge et al. propose the design optimization of the noncircular gears used in press drives, by using an eccentrically mounted circular driving gear [1], inducing a significant reduction of the pressure dwell time, increased cooling and handling time and lower thermal die loading and heat transfer from the workpiece into the dies. Mundo et. al. propose a modified crank-slider mechanism of a pressing machine whose ram is driven, according to an optimized law motion, by a pair of noncircular gears [2]. Quintero et. al. present a novel modified

crank-slider mechanism of an internal combustion engine, by introducing a noncircular gear pair [3], that improves the engine performance. Yokoyama et.al. use a pair of noncircular gear, as transmission gears secured between a power shaft and a crank shaft at a powder compacting press [4], in order to get a long powder feeding time and a longer time for compacting. All above mentioned studies are focused on the kinematics optimization of the crank-slider mechanism in order to improve the technological conditions or to reduce the production costs.

As regards the noncircular gears meshing process, few studies are mentioned in the literature [5-7], where authors have developed theoretical investigations by manipulating virtual models and using the CAD facilities.

The objectives of the paper are:

(i) defining a noncircular gear train kinematics that could be transferred to a conventional crank-slider mechanism of a nail machine, in order to optimize the nail forming process, i.e. to reduce the slider velocity, in terms of both its maximum value and variation during the nail head forming phase and the free-running phase, respectively;

(ii) generating a noncircular gear train, based on the predefined kinematics. Two gear trains are

produced as function generators for the crank-slider mechanism with modified kinematics that exhibits (a) optimum slider velocity during the nail head forming phase and (b) optimum slider velocity during the nail head forming phase and reduced velocity variation during the free-running phase, in accordance to the nail machine technological parameters;

(iii) analyzing the influence the noncircular gears geometry has on the gears tooth static contact pattern, as one of the qualitative parameters of the gears meshing.

The noncircular gears generation and mesh are developed in AutoCAD graphical environment by using original AutoLISP codes and specific drawing and editing operations.

2. THE NONCIRCULAR GEARS AND CRANK-SLIDER MECHANISM KINEMATICS

The first objective of the paper is to use a noncircular gear train in order to drive the crank-slider mechanism from the MCC337 nail machine, with the aim of optimizing the slider speed during the nail forming process. Analyzing the schematic representation of the mechanisms in figure 1, the input parameter is the noncircular gears transmission ratio $i_{21}(\varphi_1)$ that leads to a variable rotational motion for the driven gear and crank, respectively, and to a further variable translational motion of the slider; the chosen output parameter of the mechanisms is the relative velocity $dx/d\varphi_1$, where x is the slider displacement and φ_1 - the

angular parameter of the noncircular driving gear rotational motion.

Defining the gear transmission ratio, the rotational angle of the driven gear and crank, respectively, implies the following relation:

$$\varphi_2(\varphi_1) = \int_0^{\varphi_1} i_{21}(\varphi) d\varphi \quad (1)$$

The slider displacement is further expressed by:

$$s(\varphi_2) = -r \cdot \cos \varphi_2 + \sqrt{l^2 - r^2 \cdot \sin^2 \varphi_2} \quad (2)$$

where r is the crank length and l - the connection rod length.

Considering equations (1), (2), the slider relative velocity is defined by:

$$v_r(\varphi_1) = \frac{ds}{d\varphi_1} = \left[r \cdot \sin \varphi_2 \left(1 - r \cdot \sin \frac{\varphi_2}{\sqrt{l^2 - r^2 \cdot \sin^2 \varphi}} \right) \right] \cdot i_{21} \quad (3)$$

In case of the conventional crank-slider mechanism, whose rotational motion is achieved from a standard spur gear train with a constant and unitary transmission ratio, the slider displacement and the relative velocity vary as shown in figure 2 (curves s^c , v_r^c).

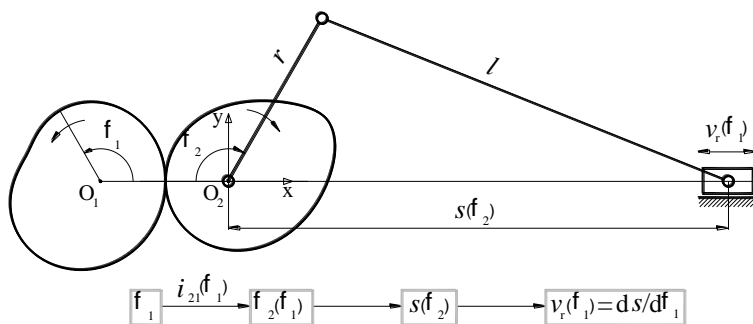


Fig. 1. The kinematics of the noncircular gears and crank-slider mechanisms

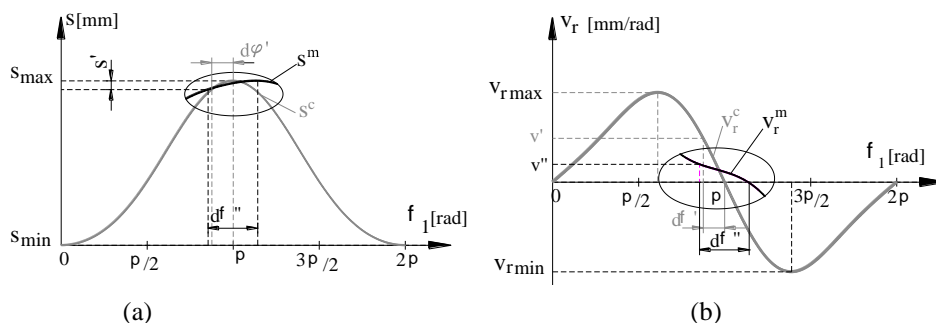


Fig. 2. The slider displacement (a) and relative velocity (b)

The optimization of the slider kinematics, as regards the nail forming process, introduces modified curves (s^m , v_r^m) and refers to a reduction of the relative velocity variation during the nail head forming phase (Fig. 2b – curve v_r^m locally substitutes the conventional curve v_r^c), a prolonged time for the forming forces action (Figs. 2a, 2b – the conventional interval $d\varphi'$ is increased to $d\varphi''$) and a reduction of the velocity variation during the free-running phase; these would improve the quality of the final product, increase the process stability and assure a low-noise production. For this purpose, the gear transmission ratio is defined as a hybrid function, with multiple parameters whose variations enable the desired crank kinematics to be chosen and noncircular gears design requirements to be satisfied.

2.1. Improving kinematics of the nail head forming phase

To improve the crank-slider mechanism kinematics during the nail head forming phase, the noncircular gear transmission ratio, as initial design data within the above mentioned algorithm, is defined by a hybrid trigonometric function, as follows:

$$i_{21}(\varphi_1) = \begin{cases} \frac{(a+b)}{2} + \frac{(b-a)\cos\left(\frac{\pi\varphi_1}{\varphi_0}\right)}{2}, \\ \varphi_1 \in [0, \varphi_0]; \\ \frac{(a+b)}{2} - \frac{(b-a)\cos\frac{\pi(\varphi_1 - \varphi_0)}{2\pi - \varphi_0}}{2}, \\ \varphi_1 \in (\varphi_0, 2\pi]. \end{cases} \quad (4)$$

where a , b are positive parameters that define the limits of the transmission ratio variation; φ_1 - the driving gear rotational angle, varying as $\varphi_1 \in [0, 2\pi]$ during the functioning cycle; φ_0 - a variable angle that splits the functioning cycle into two phases: (i) the quick advance of the wire and (ii) the nail head forming followed by the iddle phase. The above expression ensures a positive, continuous, derivative and periodical transmission ratio, as required by the theory of the noncircular gears design.

Using equation (1), the driven gear rotational angle is calculated as:

$$\varphi_2(\varphi_1) = \begin{cases} \frac{(a+b)\varphi_1}{2} - \frac{\frac{1}{2}(b-a)\varphi_0 \sin\left(\frac{\pi\varphi_1}{\varphi_0}\right)}{\pi}, \\ \varphi_1 \in [0, \varphi_0]; \\ \frac{(a+b)}{2} + \frac{(b-a)(2\pi - \varphi_0)}{2} \sin \frac{\pi(\varphi_1 - \varphi_0)}{2\pi - \varphi_0}, \\ \varphi_1 \in (\varphi_0, 2\pi]. \end{cases} \quad (5)$$

The above expression assures a positive, continuous and increasing function for the driven rotational angle. To ensure closed centrodes, the parameters should satisfy the relation: $a + b = 2$.

2.2. Improving kinematics of the nail forming process

A further improvement of the nail forming process kinematics is focused on the slider relative velocity during the free-running phase. For this purpose, the functioning cycle is divided into three phases: (i) the quick advance of the wire, (ii) the nail head forming phase and (iii) the iddle phase. Therefore, a new function is introduced to define the noncircular gears transmission ratio:

$$i_{21}(\varphi_1) = \begin{cases} \frac{(a+b)}{2} - \frac{(b-a)\cos\left(\frac{\pi\varphi_1}{\varphi_{1a}}\right)}{2\pi}, \\ \varphi_1 \in [0, \varphi_{1a}]; \\ \frac{(a+i_0)}{2} - \frac{(i_0 - a)\cos\frac{\pi(\varphi_1 - \varphi_{1a})}{\varphi_{1r} - \varphi_{1a}}}{2}, \\ \varphi_1 \in [\varphi_1, \varphi_{1r}]; \\ \frac{(b-i_0)}{2} - \frac{(b-i_0)\cos\frac{\pi(\varphi_1 - \varphi_{1r})}{2\pi - \varphi_{1r}}}{2}, \\ \varphi_1 \in [\varphi_{1r}, 2\pi] \end{cases} \quad (6)$$

where a , b are positive parameters that define the limits of the gear transmission ratio variation; i_0 – an arbitrary value of the transmission ratio, specific to the point where the nail head forming is ended, $i_0 \in [a$,

b]; φ_1 - the driving gear rotational angle, varying as $\varphi_1 \in [0, 2\pi]$ during the functioning cycle; φ_{1a} , φ_{1r} - angles that split the functioning cycle into the above mentioned three phases. The equation (6) defines a transmission ratio that is a positive, continuous,

$$\varphi_2(\varphi_1) = \begin{cases} \frac{(a+b)\varphi_1}{2} - \frac{(b-a)\varphi_{1a} \sin \frac{\pi\varphi_1}{\varphi_{1a}}}{\pi}, \\ \varphi_1 \in [0, \varphi_{1a}]; \\ \frac{(a+i_0)\varphi_1}{2} + \\ \frac{(i_0-a)(\varphi_{1r} - \varphi_{1a}) \sin \frac{\pi(\varphi_1 - \varphi_{1a})}{\varphi_{1r} - \varphi_{1a}}}{\pi} + \\ \frac{(b-i_0)\varphi_{1a}}{2}, \varphi_1 \in (\varphi_{1a}, \varphi_{1r}]; \\ \frac{(b+i_0)\varphi_1}{2} + \\ \frac{(b-i_0)(2\pi - \varphi_{1r}) \sin \frac{\pi(\varphi_1 - \varphi_{1r})}{2\pi - \varphi_{1r}}}{\pi} + \\ \frac{(b-a)\varphi_{1r}}{2} - \frac{(b-i_0)\varphi_{1a}}{2}, \\ \varphi_1 \in (\varphi_{1a}, \varphi_{1r}]; \end{cases} \quad (7)$$

Closed gears pitch curves are generated if:

$$b[2\pi - (\varphi_{1r} - \varphi_{1a})] + m_i(2\pi - \varphi_{1a}) + a\varphi_{1r} = 4\pi \quad (8)$$

3. GENERATING NONCIRCULAR GEARS BY KINEMATIC HYPOTHESIS

To generate the noncircular gears whose transmission ratio is predefined, the noncircular gears conjugate pitch curves and the teeth flanks profiles should be modelled. Based on the mating centrodes theory [8], the gears pitch curves are defined as polar curves:

$$\begin{aligned} r_1(\varphi_1) &= \frac{A}{1 + i_{21}(\varphi_1)}, \\ r_2(\varphi_2(\varphi_1)) &= A \frac{i_{21}(\varphi_1)}{1 + i_{21}(\varphi_1)}, \end{aligned} \quad (9)$$

where φ_1 is the driving centrode polar angle, φ_2 - the driven centrode polar angle, varying in accordance with equation (1) and A - the center distance.

For the gear teeth flanks generation, an analytical procedure is applied (Fig. 3), that

derivative and periodical function. The driven gear rotational angle (equation (1)) is calculated as a continuous, derivative and monotonically increasing function, by:

considers the tooth flank profile as the set of the intersection points F_{ij} between the standard rack-cutter tooth operating flank and the current line of action $(la)_{ij}$; the current line of action is inclined by a constant α pressure angle, related to the local tangent $(tg)_{ij}$ - the rolling direction, that passes through the instantaneous center of rotation P_{1ij} . The equations that describes the noncircular driven gear tooth are:

$$\begin{aligned} x_{1ij} &= r_1(\varphi_{1ij}) \cos \varphi_{1ij} \pm \\ &\pm s_{ij} \cos \alpha \cos(\mu_{ij} + \alpha + \varphi_{1ij}), \\ y_{1ij} &= r_1(\varphi_{1ij}) \sin \varphi_{1ij} \pm \\ &\pm s_{ij} \cos \alpha \sin(\mu_{ij} + \alpha + \varphi_{1ij}), \end{aligned} \quad (10)$$

where r_{1ij} , φ_{1ij} are the polar coordinates of the instantaneous center of rotation P_{1ij} , s_{ij} - the rolling distance along the current tangent line $(tg)_{ij}$, μ_{ij} - the angle of the current tangent relative to the positioning vector O_1P_{1ij} ; α - the standard pressure angle; (-) sign is for the gear tooth flank addendum points and (+) sign is for the dedendum points, when the rolling is counter clockwise.

Similar equations are written for the driving gear tooth conjugate flank points. Considering the gears meshing (Fig. 4) and using the coordinate transformation, the driven gear conjugate tooth flank is expressed, within its fixed coordinate system, as:

$$\begin{aligned} \begin{pmatrix} x_{2ij} \\ y_{2ij} \end{pmatrix} &= \begin{pmatrix} \cos \varphi_{2ij} & \sin \varphi_{2ij} \\ -\sin \varphi_{2ij} & \cos \varphi_{2ij} \end{pmatrix} \cdot \\ \cdot \left[\begin{pmatrix} -A \\ 0 \end{pmatrix} + \begin{pmatrix} \cos \varphi_{1ij} & \sin \varphi_{1ij} \\ -\sin \varphi_{1ij} & \cos \varphi_{1ij} \end{pmatrix} \cdot \begin{pmatrix} x_{1ij} \\ y_{1ij} \end{pmatrix} \right] \end{aligned} \quad (11)$$

where φ_{2ij} is the driven gear corresponding to the rotational angle, calculated by equation (1).

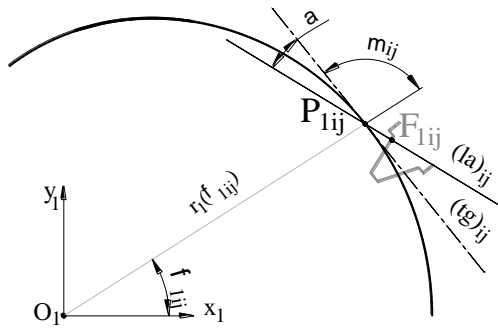


Fig. 3. The gear tooth flank generation

To generate the gears solid models, the AutoCAD application is used; the teeth flanks are automatically drawn by original AutoLISP codes and further editing operations, such as delimiting the tooth height and filleting the tooth root. Once the gears sections are completed, the virtual gears are generated by simple extrusion.

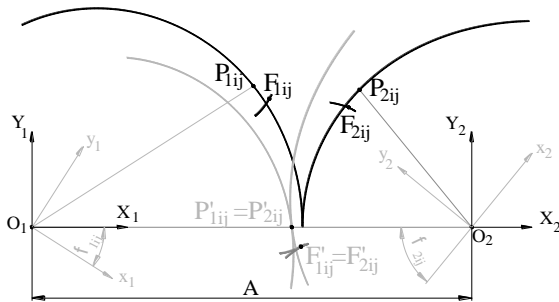


Fig. 4. The driven gear conjugate flank generation

4. SIMULATING GEARS MESH

Using the virtual solid gears, their mesh is simulated, under static conditions, and the tooth contact pattern is analyzed, especially for the teeth that are placed in zones where the gears pitch curves geometry changes its analytical definition. To produce the tooth contact, a simple algorithm is applied: (i) the gears are rotated since the analyzed teeth pair gets into mesh; (ii) a minimum gears interference is produced, by a further insignificant rotation of the driving gear, while the driven gear is fixed. This means that an extremely reduced torque is applied, in order to produce the gear interference. The tooth deflection, induced by this minimum torque, is ignored; (iii) incremental rotational motions are performed by the driving and the driven gear, respectively; each position leads to the solids interference that illustrates the number of teeth in contact and enables measurements of the tooth contact area.

It is obvious that the results are directly influenced by both the accuracy of the gears generation and the amount of the initial gears interference, but the gears mesh is mainly chosen as a qualitative parameter within the analysis of the

influence the gears kinematics have on the gears performances.

5. NUMERICAL RESULTS AND DISCUSSION

5.1. Defining the noncircular gears kinematics

In order to achieve the desired slider velocity variation during the nail forming process, based on the analysis developed in section 2, the following parameters have been chosen to define the transmission ratio (equations (4), (6)): the minimum and maximum values $a = 0.4$ and $b = 1.6$, respectively, the splitting angle $\varphi_0 = 8\pi/9$, in the case of the two phases divided functioning cycle, the splitting angles $\varphi_{1a} = 8\pi/9$ and $\varphi_{1r} = 3\pi/2$, in case of the three phases divided functioning cycle. The crank-slider mechanism geometry is defined by 150 mm and 350 mm crank and rod lengths, respectively. As seen in Fig. 5, the use of the noncircular gears leads to a slider relative velocity that is slowed down in the vicinity of $\varphi_1 = \pi$, while the nail head forming process is achieved, and is slightly increased in maximum values, compared to conventional crank drive; a reduction of the maximum reverse velocity is possible dividing the functioning cycle into three phases (Fig. 5b).

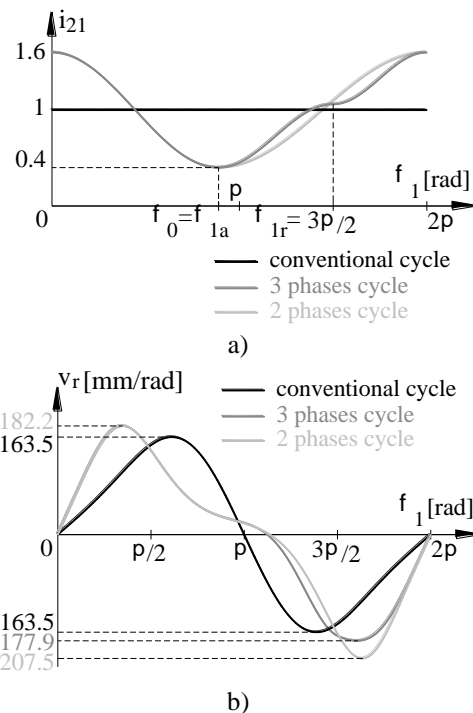


Fig. 5. The noncircular gears transmission ratio (a) and the induced slider's relative velocity (b)

5.2. Noncircular gears generation

Based on the previously mentioned transmission ratio, noncircular gears solid models

(figure 6) are generated, considering the driving and driven gears number of teeth $z_1 = z_2 = 36$, the center distance $A = 174$ mm, the pressure angle $\alpha = 20^\circ$, and the gears facewidth $B = 20$ mm.

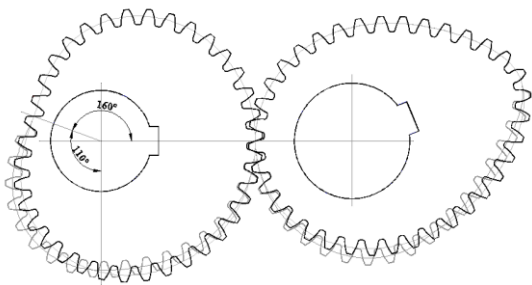


Fig. 6. The noncircular gears solid models

The gears addendum and dedendum curves are offsetting the pitch curve by $1m$ and $1.25m$, respectively, where the gears modulus, m , results as function of the pitch curve length and the gears number of teeth. The fillet radius for the tooth root is chosen at $0.38m$. As noticed from figure 6, the gear train geometries are not significantly modified by splitting the functioning cycle into two and three phases, respectively; the three phases divided cycle leads to a pair of gears with a slightly increased pitch curve curvature and length, to small changes in the gears teeth positions and flank profiles geometries, respectively, in both third and fourth quadrants.

5.3. Gears contact analysis

To analyze the influence of both modified kinematics and geometry on the noncircular gears mesh, the tooth contact pattern is investigated following the algorithm presented in section 4. An initial interference is chosen for a pinion rotational angle of 0.005° ; the noncircular pinion is incrementally rotated by $\Delta\varphi_1 = 1^\circ$, and the driven gear is rotated by the calculated $\Delta\varphi_2$ (equation (1)). The virtual solids are intersected at each position and the area of the resulted solid is measured, recording both its total and partial values, for all teeth in contact and for the main tooth being analyzed, respectively.

Figure 7 illustrates the noncircular gears, designed for the modified crank-slider mechanism kinematics, highlighting the pairs of teeth that are placed in zones where the gears geometries are changed due to a different transmission ratio. The teeth pair D1 has its operating flanks composed by two profiles, in accordance to the gear pitch curve geometry defined by equations (4), (5), (9), for a two phase divided functioning cycle, and by equations (6), (7), (9), for the three phase divided functioning cycle, respectively. The teeth pair D27 has a single curve profile, in case of two phase

kinematics, and a composed profile, in accordance to equations (6), (7), (9).

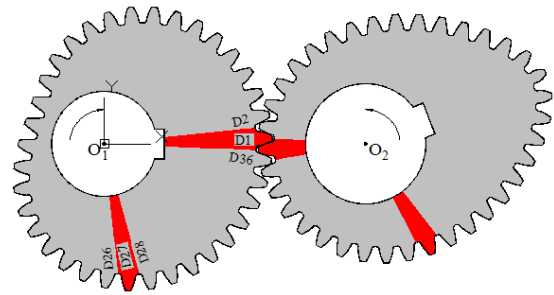


Fig. 7. Teeth selected for the mesh analysis

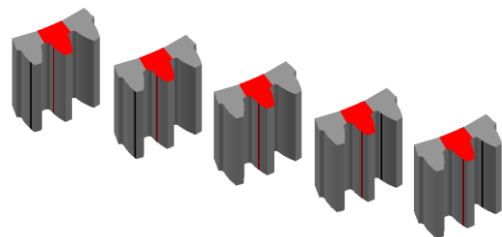


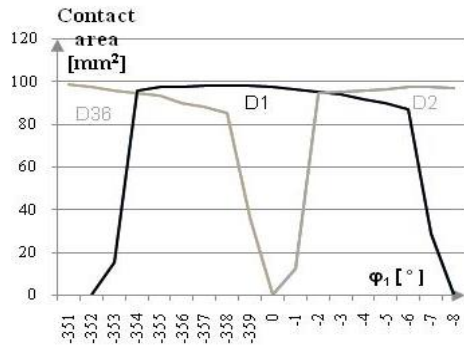
Fig. 8. Evolution of the tooth contact pattern in static mesh

Figure 8 illustrates several positions of the D1 teeth pair, while in mesh, with the contact pattern highlighted along the gear facewidth. The incremental solids intersect operation also validated the gear tooth correct generation and mesh, as no additional interferences occurred on the teeth opposite flanks.

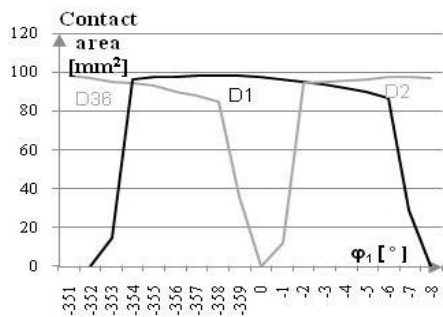
Analysing the data recorded for the D1 teeth pair mesh (Fig. 9), it can be noticed that the tooth contact pattern area and distribution are similar for the gears trains defined by equations (4) and (6). During the D1 mesh, there are always two pairs of teeth in contact, except when the tooth contact point coincides with the instantaneous center of rotation and the D1 teeth pair is single in mesh. The D1 pair gets into mesh earlier in case of the two phase divided cycle (figure 9a), by an angle of about 1° , due to the difference in tooth root position.

The behaviour of D27 tooth pair, while in contact, could be analyzed from figure 10. Due to a reduction in the pitch curve curvature within the fourth quadrant, a delay of about 4° for the tooth getting into mesh is recorded in case of the three phases functioning cycle. The gear geometry, in this case (figure 10b), is less favourable to the gear contact performances, the tooth contact area varies in a particular manner, due to the composed tooth flank profile geometry, and the tooth pair is single in mesh for about 2° rotational angle of the driving gear. Still, measuring and comparing the total contact area while D27 teeth pair is in mesh, measured along the gears teeth D26, D28 (Fig. 11), it is revealed that adjusting the gears kinematics by the third phase of the functioning cycle, the gears

induced geometry leads to a uniform distribution of the tooth contact pattern, with an increased area of contact, compared to the two phase cycles.

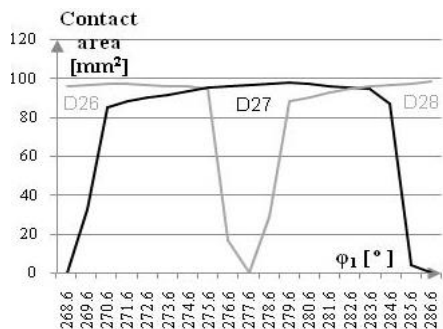


a)

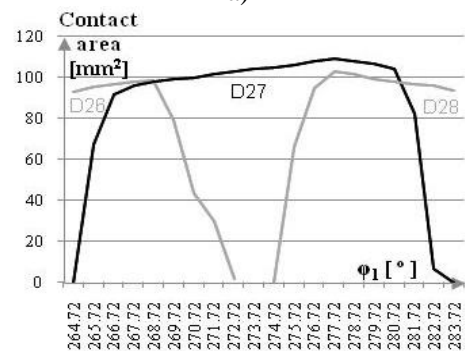


b)

Fig. 9. Areas of teeth contact patterns during the D1 tooth meshing, in case of two (a) and three (b) phases divided functioning cycle



a)



b)

Fig. 10. Areas of teeth contact patterns during the D27 tooth meshing, in case of two (a) and three (b) phases divided functioning cycle

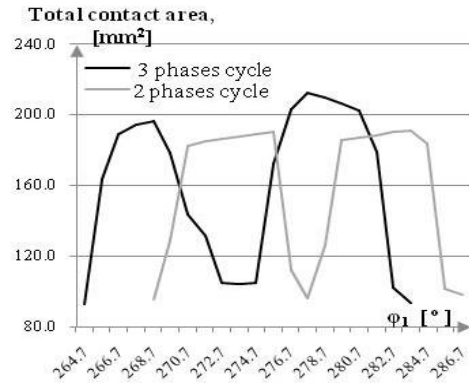


Fig. 11. Total contact area on teeth D26, D27, D28 during the D27 tooth mesh

6. CONCLUSIONS

The paper introduces a modified kinematics for the crank-slider mechanism of a nail machine, with the aim of improving the nail head forming process. Two kinematics is considered by dividing the functioning cycle into two and three phases, respectively, each kinematics being provided by a noncircular gear train. The generation of the noncircular gears, developed by kinematics hypothesis and based on the conjugate centrodes theory, for the gear pitch curves modeling, and on the rolling method for the gears tooth flanks analytical definition, enabled the gears tooth contact to be described and analyzed. The simulation of the gears mesh, performed in AutoCAD, highlighted the tooth contact pattern distribution and area. It was shown that, by dividing the functioning cycle into two phases, the gear geometry exhibited reduced curvatures, the teeth geometry induced a better contact performances as regards the contact path distribution. The three phases divided cycle implied slightly higher curvatures for the gear pitch curves, a variable composed geometry for more tooth flanks profiles, an increased rotational angle while a single tooth pair is in mesh, but, generally, a higher total tooth contact area was reported.

ACKNOWLEDGEMENTS

This work was supported by a grant of the Romanian National Authority for Scientific Research and Innovation, CNCS – UEFISCDI, project number PN-II-RU-TE-2014-4-0031.

REFERENCES

- [1] **Doege, E., Meinen, J., Neumaier, T., Schaprian, M.**, *Numerical design of a new forging press drive incorporating non-circular gears*, 2001, Proc Instn Mech Engrs 215B 465-471;
- [2] **Mundo, D., Danieli, G.A.**, *Use of the Non-Circular Gear in Pressing Machine Driving Systems*, 2004, IASME Transactions I 7-11;
- [3] **Quintero, H. F., Romero, C.A., Vanegas Useche L. V.**, *Thermodynamic and dynamic analysis of an internal combustion engine with a noncircular-gear based modified crank-slider mechanism*, 2007, 12th IFToMM World Congress Besançon ;
- [4] **Yokoyama, T., Takahashi, K.**, *Driving apparatus for powder compacting press*, 1987, US Patent 4662234;
- [5] **Khan, S.**, *Simulation and analysis of transmission error in helical non circular gear model*, 2015, Int. J. Mech. Eng. and Technol. **6** 128-136
- [6] **Barkah, D., Shafiq, B., Dooner, D.**, *3D Mesh generation for static stress determination in spiral noncircular gears used for torque balancing*, 2000, J. Mech. Design 124 313-321
- [7] **Cristescu, A., Cristescu, B., Andrei, L.**, *Finite element analysis of multispeed noncircular gears*, 2015, Appl. Mech. Mater **808** 244-251
- [8] **Litvin, F. L.**, *Noncircular Gears Design and Generation*, 2009, New York, Cambridge University Press